SCIENCE SET
OPEN ACCESS PUBLISHERS

Research Article

Global Journal of Translational Science and Integrated Technologies

Design and Analysis of a Compact Single-Stage Cavity Combiner for the 20kw Solid State Amplifier Under Vacuum

Z.H. Liu[1*], Z.G. Yin[2], Z.Y. Cheng[3], Z.Y. Xia[4], A.S. Caruso[5], & T.J. Zhang[6]

[1]*China Institute of Atomic Energy, Beijing*
[2]*National Laboratory of the South, Italy*
[3]*CNNC. Engineering Research Center of Accelerators, Beijing, China*

[*]**Corresponding author:** Z.H. Liu, China Institute of Atomic Energy, Beijing.

Submitted: 13 January 2026 **Accepted:** 23 January 2026 **Published:** 29 January 2026

Citation: *Liu, Z. H., Yin, Z. G., Cheng, Z. Y., Xia, Z. Y., Caruso, A. S., & Zhang, T. J. (2026). Design And Analy-sis of a Compact Single-Stage Cavity Combiner for the 20kw Solid State Amplifier Under Vacuum. Glo J Tran Sci & Int Tec, 2(1), 01-06.*

Abstract

Focusing on high-power acceleration systems for ultra-compact superconducting cyclotrons in special environments, we aim to make breakthroughs in key technologies that restrict the improvement of high-frequency reliability for unattended accelerators. Research has been conducted on direct power syn-thesis technology and dynamic matching adjustment for solid-state power sources at the 20kW level. A dynamically tenable single-stage cavity direct power combiner based on a TEM cavity has been designed. High-frequency power signal flow calculations have been carried out for a system with 24 inputs and 1 output. Research has also been conducted on the impact of up to three module failures at arbitrary positions on the total output of the power source under different power combining circuit topologies, as well as corresponding compensation methods. It is expected to achieve iterative breakthroughs in key technologies such as lightweight high-frequency cavity high-power direct synthesis and adaptive power amplification circuit topology reconfiguration for solid-state power sources. An adaptive, highly redundant, lightweight solid-state high-frequency power source system for space applications will be developed.

Keywords: 50 MeV, Beam Transport Line, Large Spot, High Uniformity, Scanning Magnet.

Introduction

High-frequency solid-state power sources are core equipment for particle acceleration in accelerators [1]. The main method to achieve high output power from solid-state power sources is to use power com-biners to parallel-combine the output power of mul-tiple power amplifier modules. Based on differences in the structure of combining networks, power com-bining schemes are generally divided into two types: multi-stage combining and direct combining. The 77MHz,20kW solid-state power source of the light-weight superconducting cyclotron at the China Insti-tute of Atomic Energy (CIAE) adopts a multi-stage combining scheme: first,12 two-intone power com-biners output 12 channels of 2kW power; then 2 six-in-one combiners output 2 channels of 12kW pow-er;finally,a two-in-one combiner combines the 2 channels of 12kW power to output the total power. This multi-stage combining scheme has limitations: it cannot realize online adjustment of combiner port coupling degree, leading to poor dynamic adjustment capability of output power. It also suffers from large combining loss and low efficiency [2-7].

To address these issues, this paper proposes a TEM-mode 24-in-one single-stage cavity power combiner operating at 77MHz, based on a folded λ/2 coaxial resonant cavity, with a designed output power of 20kW.This combiner adopts and cylindrical resonant cavity combining schemes in VHF or lower operat-ing frequency bands, it has smaller volume and weight, and higher structural integration. In addition, the system integrates online adaptive tuning func-tionality, which can dynamically adjust the output power of each power amplifier module. An effective output power compensation scheme is also proposed for scenarios with up to 3 module failures [8].

Research on High-Frequency Power Signal Flow in Vacuum Environment

Module Failure Analysis of Multi-Stage Combining Scheme

Taking the three-stage combining scheme mentioned in Chapter 1 as an example, we analyse the impact of module failures on total output power. We assume that all power amplifier modules and combiners are matched, and the output power phases of each mod-ule are approximately the same. Let the output volt-age of each power amplifier module be V0 and the input power be P0. Based on the microwave network characteristics of an ideal N-channel combiner:

$$V_{out} = \frac{1}{\sqrt{N}} \sum_{i=1}^{N} V_i \quad (1)$$

$$P_{out} = V_{out}^2 \quad (2)$$

We calculate the theoretical total output power of the three-stage combining scheme when 1 or 2 modules fail. The results are shown in Table 1(see Table. 1).

Table 1: Relationship Between Number/Position of Failed Modules and Output Power in Three-Stage Combining Scheme.

Number of Failed Modules	Combiner Output Power
0	24P0
1	21.98P0
2-a	19.96P0
2-b	18.23P0
2-c	16.38P0

(**Note:** a.:Two modules fail in different six-in-one bran-ches;b:Two modules fail in different two-in-one branches under the same six-in-one branch;c:Two modules fail in the same two-in-one branch.)

Research on High-Frequency Signal Flow and Failure Analysis of Single-Stage Combining Scheme

Similarly, for the 24-channel cavity combiner-based single-stage combining scheme, the transmission coefficient from the input port to the output port of the 24-channel cavity power combiner is derived from the microwave network characteristics of an ideal N-channel combiner:$S_{i,25}$=10lg1/24≈-13.80dB(i=1,2,...,24). The transmission coefficient between input ports is S_{ji}=20lg1/24≈-27.60dB(j≠i, j=1,2,...,24).Based on this and Eqs. (1)-(2),we further calculate the change in combiner output power when 1 to 3 power amplifier modules fail under ideal conditions. The results are shown in Table 2 (see Table. 2).

Table 2: Relationship Between Number of Failed Modules and Output Power in Single-Stage Com-bining Scheme.

Number of Failed Modules	Combiner Output Power
0	24P0
1	22.06P0
2	20.61P0
3	18.38P0

By analysing the impact of the number of failed modules on combiner output power in both multi-stage and single-stage combining schemes, we con-clude that the output power of the single-stage com-bining scheme is less affected by port module fail-ures. This makes it more conducive to timely ad-justment of output power in subsequent operations.

Research on High-Frequency Simulation of Cavi-ty Power Combiner in Vacuum Environment

The high-frequency simulation model of the 24-channel cavity combiner consists of a folded λ/2 coaxial resonant cavity (main body),24 input cou-plers, and 1 output coupler. The main body of the coaxial resonant cavity operates in TEM mode, with a Q-factor of 8000 and a resonant frequency of 76.98MHz—in-dicating excellent theoretical high-frequency performance of the main structure. The 24 input coupling ports are evenly distributed at both ends of the coaxial resonant cavity. Power from the power amplifier modules is coupled into the combin-er via magnetic coupling. The 24 input coupling loops are divided into three groups based on their positions. Their shapes, specific positions, and rota-tion angles are optimized through impedance match-ing simulations. The output coupling port uses a capac-itor disk coupling method to couple power to the output port. The depth of the coupling disk ex-tending into the cavity is optimized. The input ports are designed as standard 40mm high-frequency inter-faces, and the output port is designed as a standard 80 mm high-frequency interface.

After adjusting all parameters, time-domain simula-tions are performed on the model. The simulation results of the combiners transmission parameters and electric/magnetic field distribution are shown in Figs. 1-3. (see Fig. 1-3)

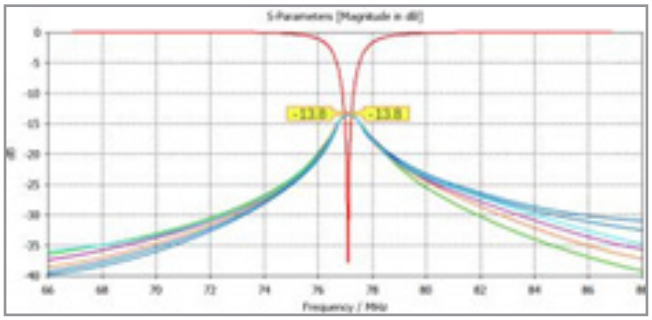

Figure 1: Simulation rresults of ccavity ccombiner ttransmission pparameters.

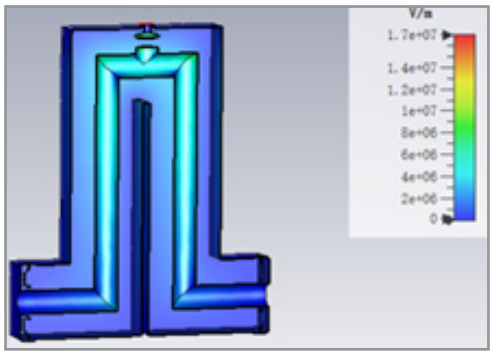

Figure 2: Electric field ddistribution inside cavity ccombiner

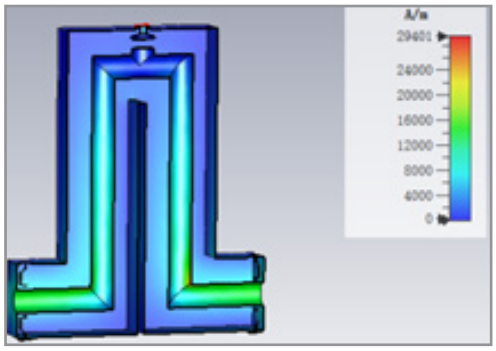

Figure 3: Magnetic fidle ddistribution inside cavity combiner.

From the transmission parameter simulation results, the cavity combiner exhibits goodtransmission char-acteri-stics and isolation between ports, indicating excellent high-frequency performance around 77MHz. The electric field distribution diagram shows small and continuous electric fields at the connection structures, confirming the overall good performance of the combiner. The simulation results verify the feasibility of the single-stage combining scheme.

Mechanical Structure Design of Cavity Combiner for Vacuum Environment

Vacuum-Adaptive Design of the Overall Combiner Structure

The overall structure of the power combiner is shown in Fig. 4(see Fig. 4), which can be divided into a housing, a frame, an inner conductor, and in-put/output coupling structures. To adapt to the vacu-um working environment: the frame is made of angle aluminum; the housing and inner conductor are made of TU1 oxygen-free copper.The frame is formed by welding angle aluminum. Copper sheets are fastened to the bracket with screws to form the housing. The housing consists of an upper cover plate and a lower main body. A 1-5/8-inch opening is designed in the middle of the upper cover plate to facilitate the in-stallation of the output coupling device. The upper cover plate is connected to the housing via screws to enable detachable functionality.

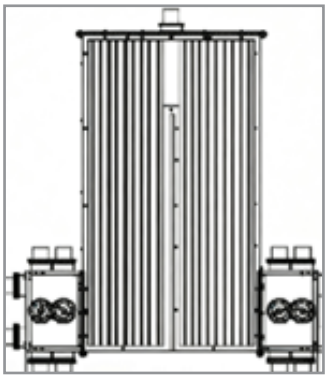

Figure 4: Schematic diagram of overall mechanical structure of combiner.

Input and Output Coupling Structure Design

To achieve rapid isolation of failed modules and flexible adjustment of output power, the input cou-pling structure adopts a dynamically tunable magnet-ic coupling design. This structure takes the input coupling loop as the core component, combined with a peripheral fixed ring, a rotary sealing device (bear-ing, oil seal), and a transmission gear to form a ro-tatable mechanism.Finger spring contact technology is used between the coupling loop and the cavity wall. This not only ensures continuous high-frequency signal transmission during rotation but also effectively reduces rotational resistance, ena-bling long-term stable electromechanical coupling of the system in a vacuum environment.Input and out-put coupling structures are shown in Figure 5(see Fig. 5)

The output coupling structure adopts tunable capaci-tor coupling technology. A motor-position sensor closed-loop control system drives the coupling ca-pacitor plate to move with precise vertical displace-ment along the guide rail. This real-time adjusts the distance between the capacitor plate and the inner surface of the

cavity, thereby changing the coupling capacitance. This design enables online adjustment of the output coupling degree according to actual working conditions (e.g., changes in the number of modules, load impedance fluctuations).

Compared with traditional fixed coupling methods, this mechanical design with dynamic tunability at both input and output ends allows the combiner to not only quickly decouple failed modules but also realize adaptive adjustment of output power when modules fail. This significantly improves the unat-tended reliability of the solid-state power source in a vacuum environment.

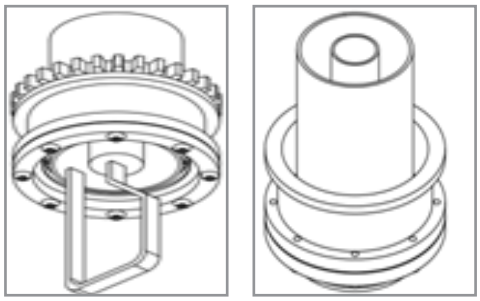

Figure 5: Input coupling structure and output cou-pling structure.

Electronic Design of Amplitude-Phase Controller Based on Hammerstein-Wiener Nonlinear Model

Module Failure Detection and Response Scheme

To realize real-time monitoring of the operating sta-tus of power amplifier modules and rapid isolation of failures, a directional coupler is configured at the output end of each power amplifier module. This coupler extracts forward power and reflected power information of the output signal. Meanwhile, a phase detection circuit acquires phase information of each channel, enabling non-intrusive real-time monitoring of the output power amplitude and phase of each module. The schematic diagram of module failure detection and response scheme is shown in Figure 6(see Fig. 6).

The collected analog signals are converted from ana-log to digital via a high-speed multi-channel data acquisition system and transmitted to the central amplitude-phase controller in real time. The control-ler embeds a fault diagnosis algorithm, which deter-mines the module operating status by setting a power threshold (usually 50%-60% of the rated power).

When a sudden drop in the output power of a module is detected, the system triggers a fault response pro-gram within milliseconds. After confirming the mod-ule failure, the amplitude-phase controller immedi-ately sends a control command to the motor drive unit at the combiners input port corresponding to the failed module.The drive unit uses a stepper motor or servo motor to drive a precision gear transmission mechanism, rotating the input coupling loop to a position orthogonal to the magnetic field inside the cavity (coupling degree approaching 0dB). This real-izes electrical isolation between the failed module and the combiner cavity, preventing the failed mod-ule from affecting other normally operating modules and ensuring overall system stability.

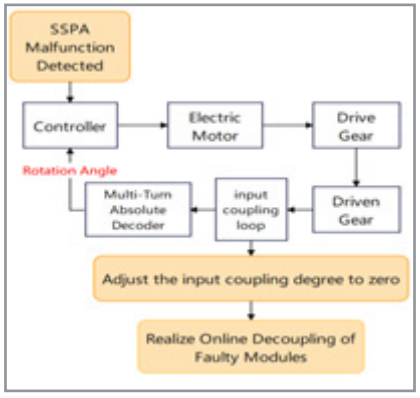

Figure 6: Schematic diagram of module failure detection and response scheme.

Online Coupling Degree Adjustment and Power Compensation Scheme

After decoupling the failed module, the total output power of the cavity combiner will decrease signifi-cantly. The magnitude of the power drop can be es-timated with reference to Table 2. To restore the out-put power to the set value in the shortest time, dy-namic power compensation for the remaining nor-mally operating modules is required. This study pro-poses a compensation scheme based on the Hammer-stein-Wiener nonlinear model for amplitude-phase control. The specific implementation steps are as follows:

1. Measurement of Power Amplifier Characteristic Curves

The input-output nonlinear characteristic curves of 24 power amplifier modules are measured. The Hammerstein-Wiener nonlinear model is used to fit the test data, obtaining the corresponding pre-distortion function. On this basis, a lookup table (LUT) of the excitation signal size and the output power amplitude/phase of the power amplifier mod-ules is established.

2. Online Power Compensation Algorithm

When a significant drop in combiner output power is detected, the amplitude-phase controller calculates the power deficit and adopts a uniform distribution strategy to evenly allocate the re-

quired compensation power to the remaining power amplifier modules.

The controller retrieves the pre-established LUT to reversely calculate the excitation signal power re-quired to achieve the target output power. It then adjusts the power of the power amplifier modules by changing the size of the excitation signal. Mean-while, considering the phase changes that may be caused by power adjustment, the controller synchro-nously adjusts the phase pre-compensation value of each module. This ensures that the signals at all input ends are superimposed in phase, maintaining optimal combining efficiency.

The block diagram of the power compensation scheme is shown in Fig.7(see Fig. 7), illustrating the complete control process from fault detection and module decoupling to power compensation.

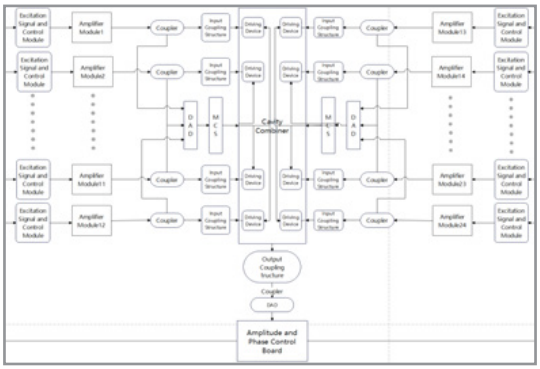

Figure 7: Output power compensation scheme block Diagram.
(**Note:** In this figure, MCS means Motor Control Sys-tem,DAD means Data Acquisition Decive.)

Vacuum Test Scheme for Solid-State Power Source-Combiner

The block diagram of the joint vacuum environment test system for the 20kW solid-state power source and power combiner is shown in Fig.8(see Fig. 8). To achieve optimal combining efficiency during power combining, all power amplifier plug-ins of the solid-state power source must undergo independent vacuum environment tests before the joint test. These tests acquire parameters such as the output power amplitude and phase of the power amplifier plug-ins under vacuum conditions. Based on the test data, the amplitude and phase of all power amplifier plug-ins are adjusted to be basically consistent. Analysis of the vacuum environment test data of a single power amplifier plug-in of the 20kW solid-state power source shows that the operating status of the circulator has a significant impact on the output power characteristics of the power amplifier plug-in. Therefore, the amplitude and phase of the output power of the power amplifier plug-in can be adjusted by regulating the operating voltage of the circulator to change its S-parameters. The 20kW solid-state power source and vacuum test tank physical image is shown in Figure 9(see Fig. 9)

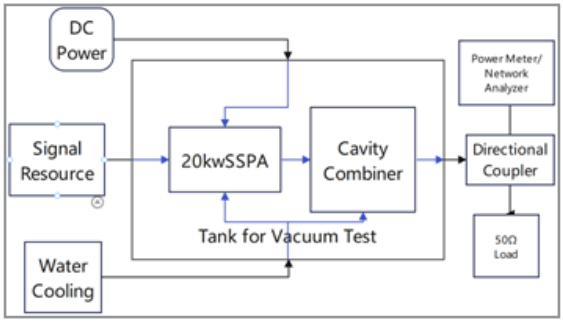

Figure 8: Vacuum test block diagram

Figure 9: 20kW solid-state power source and vacu-um test tank physical image.

Conclusions and Prospects

This paper addresses issues such as poor dynamic adjustment capability of output power and low com-bining efficiency in the existing power combining scheme of the 77MHz, 20kW solid-state power source for the CIAE lightweight superconducting accelerator. A single-stage power combining scheme with adap-

tive output power adjustment is proposed, and the main progress is as follows:

1. A TEM-mode 24-in-one single-stage cavity power combiner based on a λ/2 coaxial resonant cavity is designed. The feasibility of the scheme is verified through high-frequency simulations, making it suita-ble for VHF or lower frequency bands.
2. The mechanical structures of the main body, input couplers, and output coupler of the 24-channel cavity power combiner are designed. Corresponding opti-mizations are made for its application in a vacuum environment.
3. Research on the high-frequency power signal flow of the combiner is conducted. The impact of up to 3 module failures (at arbitrary positions) on the total output power of the combiner under different com-bining circuit topologies, as well as corresponding compensation methods, are studied.

In the next step, cold test and debugging of the man-ufactured cavity combiner prototype will be carried out, along with power testing in a vacuum environ-ment. Meanwhile, research on adaptive amplitude-phase control algorithms and hardware under power amplifier module failure conditions will be initiated.

References

1. Sun, Y., & Gao, S. (2020). A high-power combiner based on folded λ/2 coaxial cavity for VHF band. IEEE Transactions on Mi-crowave Theory and Techniques, 68(5), 1852–1860. https://doi.org/10.1109/TMTT.2020.2977775
2. Li, Y., Wang, X., & Zhang, Z. (2022). High-efficiency single-stage power combin-ing using folded coaxial resonant cavities at VHF band. IEEE Transactions on Micro-wave Theory and Techniques, 72(1), 818–821. https://doi.org/10.1109/TMTT.2022.3187654
3. Jiang, G., Shi, L., Sun, L., Jin, K., Wu, Z., Huang, G., & He, Y. (2021). Design of cav-ity power combiner with rotatable online decoupling system. High Power Laser and Particle Beams, 33(5), 343–352. https://doi.org/10.11884/HPLPB202537.240257
4. Smith, J., Brown, A., & Jones, R. (2022). Adaptive impedance matching for high-power solid-state amplifier arrays. IEEE Transactions on Power Electronics, 55(12), 5890–5901. https://doi.org/10.1515/cclm-2017-0008
5. Chen, H., Liu, L., & Guo, W. (2022). Cy-lindrical resonant cavity–based power com-biners for multi-kW SSPA systems. Inter-national Journal of RF and Microwave Computer-Aided Engineering. https://doi.org/10.1002/mmce.220012
6. Kim, K., Lee, S., & Park, J. (2001). Fault-tolerant power combining architectures with real-time compensation for accelerator systems. Nuclear Instruments and Methods in Physics Research Section A, 998, Article 165321. https://doi.org/10.1016/0883-2889(91)163521
7. Wu, C., Yang, Y., Huang, Z., Tripathi, N. M., Kalman, H., & Levy, A. (2021). Minia-turized coaxial resonant cavities for high-power microwave applications. Applied Physics, 225, 130–172. https://doi.org/10.1063/5.0064789
8. Garcia, M., Sanchez, P., & Gonzalez, D. (2017). Low-loss multi-stage power combin-ing networks for particle accelerator drivers. Physics Procedia, 87, 45–52. https://doi.org/10.1016/j.phpro.2017.05.007